CrossMark

Turbidity patterns of spontaneous peptidization in an aqueous abiotic system and possible secondary peptide structures

A. Maciejowska[1] · A. Godziek[1] · M. Sajewicz[1] ·
T. Kowalska[1]

Abstract The non-linear dynamics of spontaneous peptidization running in 10 monocomponent and binary abiotic liquid systems of *L*- and *D*-Ala and *L*- and *D*-Phe is investigated with use of turbidimetry with continuous registration, high-performance liquid chromatography with light scattering detection (HPLC-ELSD), mass spectrometry (MS), and spectroscopy of far UV circular dichroism (CD). The turbidity patterns represent a sum of the light scattering effects caused by insoluble peptides of unknown yields, structures, and molecular weights. The auxiliary analytical techniques confirm the non-linear nature of peptidization (HPLC-ELSD) and spontaneous formation of the homo- and heteropeptides (MS). CD spectroscopy seems to confirm the presence of the secondary α-helix structures. The similarity of turbidity patterns is revealed with the monocomponent (*L* or *D*) and binary (*L-L* or *D-D*) systems of equichiral α-amino acids, and dissimilarity of patterns is observed with the binary systems of inequichiral α-amino acids (*L-D*). The tentative conclusion is drawn that the peptides assembled of equichiral α-amino acid units are able to assume the secondary (right- or left-handed α-helix) structures, which in a certain way could foster the similarity of turbidity patterns, and the peptides built of inequichiral α-amino acid units cannot ensure an efficient enough stringing of monomer molecules into equichiral heptades to form complete segments of an α-helix. This randomness of the α-amino acids arrangement in the inequichiral peptide molecules most probably manifests itself as a lack of similarity among the respective turbidity patterns.

✉ T. Kowalska
teresa.kowalska@us.edu.pl

[1] Institute of Chemistry, University of Silesia, 9 Szkolna Street, 40-006 Katowice, Poland

Introduction

Spontaneous non-linear formation of peptides from the monomeric and optically pure α-amino acids running in the abiotic liquid systems in parallel with spontaneous non-linear chiral conversion was first reported in papers [1–3]. In fact, these two non-linear processes have not been observed with α-amino acids alone, but with a wider selection of the low molecular weight chiral carboxylic acids such, as profen drugs [4, 5] and hydroxyl acids [6, 7], so it can be justifiably speculated that these two non-linear processes are even more general than our up-to-the-date understanding thereof. Below, the mechanisms are presented of chiral conversion (Scheme 1a), peptidization (Scheme 1b), and the two processes running in the parallel (Scheme 1c), upon an example of L-Ala, one of the α-amino acids which will be referred to in the experimental part of this study.

Earlier, no similar observations have been made with α-amino acids dissolved in abiotic aqueous or non-aqueous media, in the absence of a catalyst. Moreover, the selected peptide structures tend to be viewed as fairly stable units (e.g., [8–10]), often with some negative health repercussions (e.g., as a cause of the age-related neurodegenerative diseases [10–12]) or to the contrary, they can be positively employed in various different biomedical nanotechnology contexts, owing to their biocompatibility (e.g., [10, 13, 14]). Numerous reports on the lack of peptide stability in abiotic solutions refer to their decomposition (e.g., hydrolysis) rather than to their spontaneous formation (the latter process being the leitmotif of this study) and they tend to ascribe such phenomena to the external stimuli such, as pH, temperature, chemical nature of solvents, etc. [15–17].

The spontaneous non-linear peptidization of α-amino acids has been documented in our earlier studies with use of several analytical techniques, and in the first instance liquid chromatography (both HPLC and TLC) [18, 19], turbidimetry with continuous data acquisition [20, 21], and scanning electron microscopy (SEM) [22]. Although the least employed analytical technique has been turbidimetry, we consider it as well suited to tracing the dynamics of the aforementioned process, as peptidization almost instantaneously yields insoluble peptides, initially invisible to human eye. This analytical technique is appropriate to the media of rather low turbidity in which the suspended particles are small [23], which is the case in this study. Moreover, turbidimetry has already proved useful in some other investigations, and its particularly attractive feature is that it facilitates the detection of very short-lived pulsing of suspended precipitates, which characterizes many systems and reveals the precipitate mobilization processes (e.g., [24]).

The aim of this study is to trace the turbidity patterns of spontaneous peptidization in the monocomponent and binary L-Ala, D-Ala, L-Phe, and D-Phe systems, the latter ones assembled in the equichiral and inequichiral configurations, using turbidimetry with continuous registration. As the auxiliary analytical
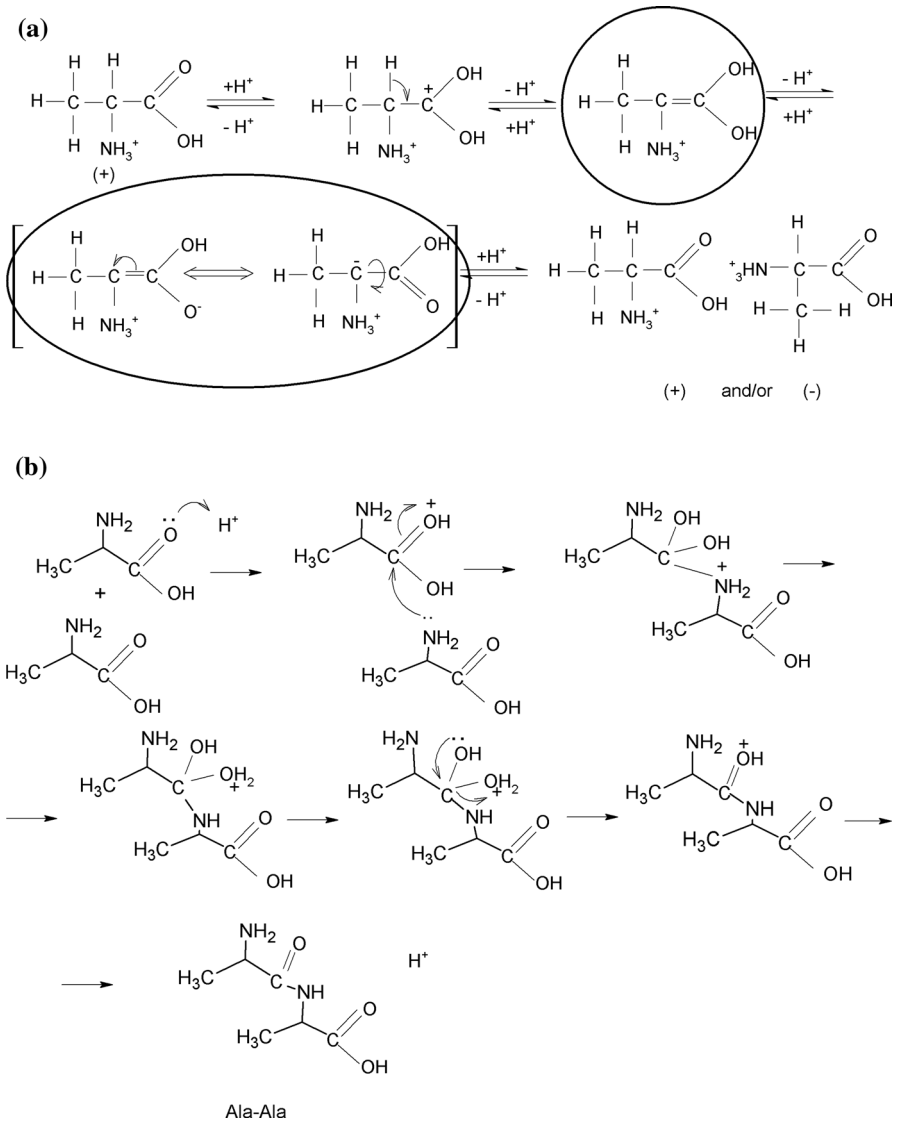
Scheme 1 Molecular mechanisms of the processes running in the monocomponent *L*-Ala system dissolved in an aqueous medium: **a** Chiral conversion of *L*-Ala to *D*-Ala (intermediary non-chiral structures are marked with *black ovals*); **b** homopeptide formation (*L*-Ala-*L*-Ala); and **c** peptidization (Ala-Ala)$_n$ running in the parallel with chiral conversion

techniques, HPLC-ELSD, MS and CD were used, in order to assess the dynamics of the investigated process, the chemical structure of the resulting peptides, and the presence of α-helices in solutions, respectively.
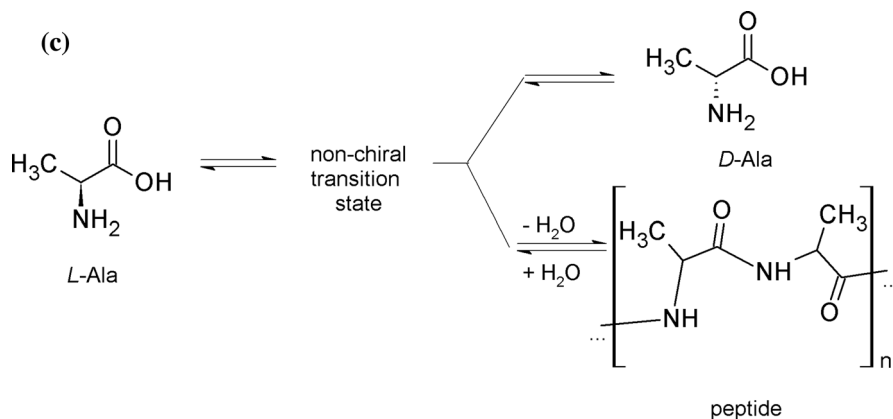
Scheme 1 continued

Experimental

Reagents

We used L-Ala and D-Phe (Reanal, Budapest, Hungary), D-Ala (Sigma-Aldrich, St Louis, MO, USA), and L-Phe (Merck KGaA, Darmstadt, Germany). All α-amino acids were of analytical purity. Methanol (Sigma-Aldrich) was of HPLC purity. Glacial acetic acid and conc. hydrochloric acid (PPH POCh, Gliwice, Poland) were of analytical purity. Water was de-ionized and double distilled in our laboratory by means of the Elix Advantage model Millipore System (Molsheim, France).

For all the experiments, concentrations of the investigated α-amino acids in the monocomponent systems were 1.0 mg mL^{-1} (i.e., 1.12×10^{-2} mol L^{-1} for L-, D-, and DL-Ala, and 6.05×10^{-3} mol L^{-1} for L-, D-, and DL-Phe), and 0.5 mg mL^{-1} (i.e., 5.61×10^{-3} for L- and D-Ala, and 3.03×10^{-3} mol L^{-1} for L- and D-Phe) in the binary systems. The 70% aqueous methanol (i.e., 70% methanol + 30% water, v/v), known for its strong antiseptic properties, was selected as a solvent in order to protect the α-amino acid solutions from microbial action in the experiments of sample ageing. Sample ageing for the purpose of all the experiments except turbdimetric analysis was carried out just by storage of samples in the transparent and tightly stoppered volumetric flasks on the laboratory shelf, with the natural illumination changes in the day/night cycle. Storage of samples for the purpose of the chromatographic analyses was at 22 ± 1 °C and for the purpose of turbidimetric analyses, at 25.0 ± 0.5 °C. Glacial acetic acid as a control sample for turbidimetric measurements was also dissolved in 70% aqueous methanol at the concentration of 1 mg mL^{-1} (1.67×10^{-2} mol L^{-1}).

Turbidimetry

Turbidity measurements were performed for 10 monocomponent and binary α-amino acid systems listed in the preceding section with use of the turbidity sensor

(TRB-BTA, Vernier Software & Technology, Beaverton, OR, USA) that allowed continuous monitoring of turbidity changes. For these experiments, *ca.* 15-mL aliquots of the amino acids solutions in 70% aqueous methanol were freshly prepared and placed in the instrument vials. The respective turbidity changes were registered for the period of 14 days (in 1-min intervals). To confirm the qualitative reproducibility of the results, the turbidity measurements were repeated twice. Moreover, the stability of turbidity measurements was controlled in the course of one day for water, methanol, and 70% aqueous methanol as the reference solvents, and the relative standard deviation (RSD) of these measurements proved very low (0.29% for pure methanol and 0.79% for 70% aqueous methanol). Similarly, turbidity measurements were carried out in the course of one day for the solution of glacial acetic acid (as a simple model of the low molecular weight non-chiral carboxylic acid) in 70% aqueous methanol and again, stability of these results was confirmed by an insignificant relative RSD value (below 0.50%).

HPLC-ELSD

The HPLC-ELSD system was used to monitor concentration changes of the six α-amino acid systems (*L*-, *D*-, and *DL*-Ala, and *L*-, *D*-, and *DL*-Phe) in the function of time. The analyses were carried out using the Varian model 920 liquid chromatograph equipped with the 900-LC autosampler, the gradient pump, the 380-LC ELSD detector, the C18 column (250 mm × 4.6 mm i.d., 5 μm particle diameter; Varian; cat. no. A3000250C046), and the Galaxie software for the data acquisition and processing. The chromatographic column was thermostatted at 35°C using the Varian Pro Star 510 column oven. Chromatographic analyses were carried out over the course of 48 h at the 10-min intervals in the isocratic mode. The 5-μL sample aliquots and the methanol–water (20:80, *v/v*) mobile phase at a flow rate of 0.8 mL min^{-1} were used.

LC-MS

Mass spectra of the four binary systems (*L*-Ala-*L*-Phe, *D*-Ala-*D*-Phe, *L*-Ala-*D*-Phe and *D*-Ala-*L*-Phe) dissolved in 70% aqueous methanol aged for four weeks were recorded with use of the Varian MS-100 mass spectrometer. The working MS conditions were the following: ESI-MS scan from *m/z* 50–2000, positive ionization, spray chamber temperature 50 °C, drying gas temperature 250 °C, drying gas pressure 25 psi, capillary voltage 50 V, needle voltage 5 kV.

Spectroscopy of far UV circular dichroism (CD)

The circular dichroism spectra in the far UV range (190 ÷ 260 nm) were registered for the monomeric and binary α-amino acid samples analogous to those used for turbidimetric measurements (i.e., for the 10 freshly prepared and 10 aged samples after the four months ageing period), yet diluted in proportion of 1: 25 (v/v) with water. The CD spectrum of the blank sample (0.20 mL 70% aqueous methanol + 4.80 mL H$_2$O) was also registered and subtracted from each spectrum

of the amino acid solution. The measurements were carried out for the samples placed in the 1-mm cell with use of the J-815 model CD spectrometer (Jasco Electronics Holdings, Johannesburg, South Africa).

Results and discussion

Turbidity patterns

Turbidimetric monitoring of spontaneous peptidization was carried out in the continuous mode (in the 1-min intervals) by the registration of the nephelometric turbidity units (NTU) for the period of 14 days at 25.0 ± 0.5 °C. The patterns of turbidity changes in the function of time are given in Figs. 1a–1c. Based on visual assessment, these patterns can be divided in two groups. Group 1 includes six different monocomponent and binary α-amino acid samples characterizing with a similarity of turbidity patterns among different samples (Figs. 1a and 1b). Group 2 includes four different binary α-amino acid samples characterizing with dissimilarity from the aforementioned six cases and from one another (Fig. 1c).

The first two cases are classified as those belonging to Group 1 (Subgroup 1a), which includes the monocomponent L-Ala and L-Phe solutions. The respective turbidity patterns look similar to one another, with an initial drop of turbidity followed by its gradual increase, to finally head toward a steady state (Figs. 1ai and 1aii). Frequent and needle-like oscillatory changes most probably have a physical meaning, as they are not artifacts caused by the power supply or temperature instability (the employed measuring system was carefully stabilized). The four cases belonging to Group 1 (Subgroup 1b) are characterized by turbidity patterns also looking similar to one another with spiky oscillations followed by an oscillation damp and the turbidity eventually heading toward a steady state. Subgroup 1b includes two monocomponent solutions (D-Ala and D-Phe, Fig. 1biii, iv) and two binary solutions (L-Ala-L-Phe and D-Ala-D-Phe, Figs. 1bv and 1bvi).

The dissimilar turbidity patterns with four binary α-amino acids solutions (DL-Ala, DL-Phe, L-Ala-D-Phe, and D-Ala-L-Phe) are classified as Group 2. With DL-Ala, after an initial turbidity drop lasting less than one day, rather insignificant oscillatory changes of turbidity are observed, very close to a steady state (Fig. 1cvii). With DL-Phe, rapid and continuous oscillatory drop of turbidity is observed (Fig. 1cviii). With L-Ala-D-Phe, an oscillatory drop of turbidity is followed by the oscillations around a steady state, to finish with a well pronounced turbidity growth (Fig. 1cix). With D-Ala-D-Phe, one observes weak and irregular oscillations of turbidity around a steady state (Fig. 1cx). A reminder can be made that the experimental turbidity patterns (characterized by spiky oscillations and then turbidity building up to a steady state) were modeled in the theoretical section of paper [25].

Let us consider possible reasons of similarity of the turbidity patterns within Group 1 (Figs. 1a and 1b) and dissimilarity within Group 2 (Fig. 1c). With solutions of four optically pure α-amino acids belonging to Group 1 (L-Ala, D-Ala, L-Phe, and D-Phe), at the initial peptidization stage, the formation of peptides built of

(a)
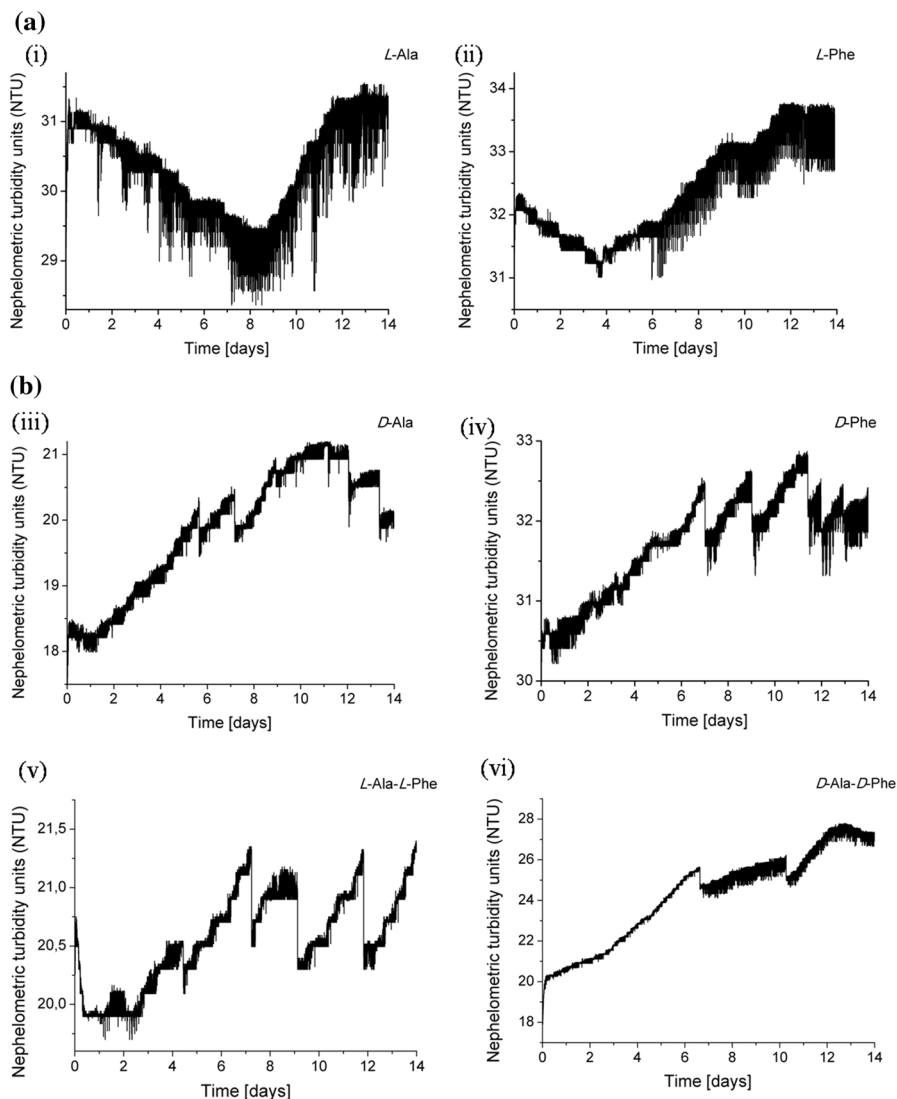
(i)

(ii)

(b)

(iii)

(iv)

(v)

(vi)

Fig. 1 Patterns of turbidity changes (in nephelometric turbidity units (NTU)) in the function of time for the solutions: **a** (i) *L*-Ala, (ii) *L*-Phe, **b** (iii) *D*-Ala, (iv) *D*-Phe, (v) *L*-Ala-*L*-Phe, (vi) *D*-Ala-*D*-Phe, **c** (vii) *DL*-Ala, (viii) *DL*-Phe, (ix) *L*-Ala-*D*-Phe, and (x) *D*-Ala-*L*-Phe

equichiral α-amino acids is expected (until spontaneous chiral conversion results in accumulation of meaningful amounts of inequichiral counterparts, which is not likely in the initial 14 days of the experiment). It is not certain if these equichiral peptides can assume the secondary α-helix structure under our experimental conditions, yet such a possibility with a consequent formation of the backbone H-bonds between the >CO of peptide group i and the >NH of peptide group $i + 3$
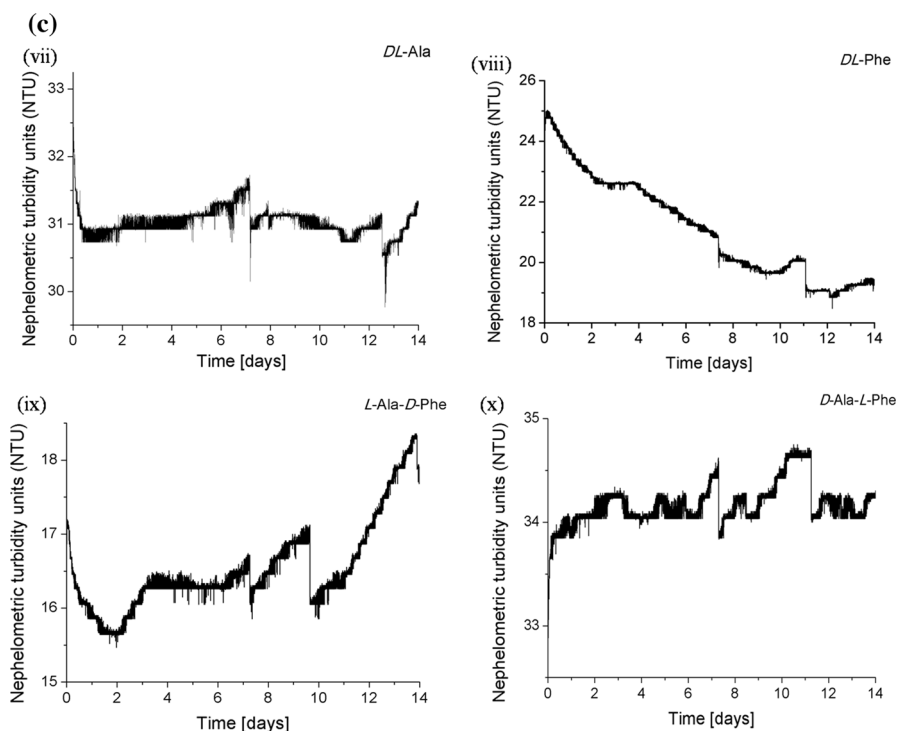
(c)

Fig. 1 continued

[26] is anticipated. One has to additionally comment on the difference between the turbidity patterns valid for *L*-Ala and *L*-Phe on the one hand (Figs. 1ai and 1aii) and those valid for *D*-Ala and *D*-Phe on the other (Figs. 1aiii and 1aiv). This difference could be due to the fact that in the former case, the right-handed α-helices are formed and in the latter case the left-handed ones [27], claimed to be somewhat less stable in an aqueous environment [28]. Indirectly, such a difference is confirmed by our earlier turbidity measurements carried out for *L*-Ser and *D*-Ser [29], where the turbidity pattern of *L*-Ser demonstrated the circadian rhythm of turbidity changes, and *D*-Ser did not show such a rhythm. Thus the difference in the handedness of the right- and left-handed α-helices can probably influence the different dynamics of peptidization and consequently, a different light-scattering effect (reflected in the difference of the respective turbidity patterns).

With the solutions of the two binary α-amino acid mixtures belonging to Group 1 (*L*-Ala-*L*-Phe and *D*-Ala-*D*-Phe, (Figs. 1bv and 1bvi), one expects formation of the homo- and heteropeptides. However, both homo- and heteropeptides can assemble in equichiral α-amino acid units, so that the right-handed (*L-L*) and the left-handed (*D-D*) α-helices can be expected as a possible reason of similarity of the respective turbidity patterns. Herewith, it needs to be added that both Ala and Phe have long been recognized among the most helicogenic α-amino acids [30].

Group 2 differs from Group 1, as it includes four binary mixtures (*DL*-Ala, *DL*-Phe, *L*-Ala-*D*-Phe, and *D*-Ala-*L*-Phe) with the opposite chiral configurations of the two counterparts (either *L-D*, or *D-L*). Although in this case both homo- and heteropeptides can be formed spontaneously, the preferential formation of heteropeptides is statistically more probable. The heteropeptides in Group 2 are built of inequichiral α-amino acid units, with a random sequence of the *L* and *D* α-amino acids. Since ∼3.5 equichiral α-amino acid units are needed per one turn in the α-helix (and the smallest integer number required to ensure two complete α-helical turns is 7 [31]), a random sequence of the *L* and *D* α-amino acid units cannot ensure an efficient enough stringing of equichiral molecules into the equichiral heptade regions (either left-, or right-handed). This randomness of the α-amino acids arrangement in the inequichiral peptide molecules most probably manifests itself as a lack of similarity among the respective turbidity patterns. The turbidimetric results valid for Group 2 indirectly strengthen our assumption as to possible formation of the α-helix structures in spontaneous peptidization with equichiral α-amino acids. However, the formation of peptide α-helices is regarded as a working hypothesis only (conceived by equichirality of the monomeric units involved), although the other molecular level mechanisms cannot be excluded which might eventually complement or replace the α-helix concept.

As controls, we present the time dependence of the turbidity for water, methanol, 70% aqueous methanol and the glacial acetic acid solution in 70% aqueous methanol over 24 h (Fig. 2). Stable turbidity values for the three solvents and the solution of acetic acid (as a simple model of the low molecular weight non-chiral carboxylic acid) apparently differ from the dynamic behavior of the α-amino acid solutions. We interpret increases in turbidity to correspond to the growing amounts of the nano- and microparticles suspended in the solution, owing to the progress of peptidization (because from our partially unpublished experiments performed with use of the scanning electron microscopy, it comes out that insoluble peptides are
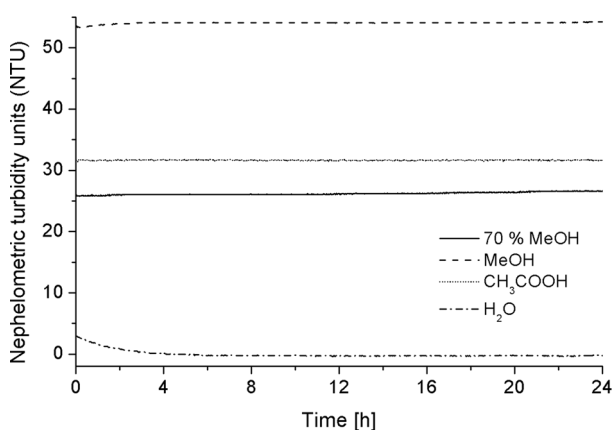

Fig. 2 Turbidity (in nephelometric turbidity units, NTU) for water (H_2O), methanol (MeOH), 70% aqueous MeOH, and 1 mg mL^{-1} solution of glacial acetic acid in 70% aqueous MeOH registered for 24 h

formed almost instantaneously in the solution, much earlier than they can be perceived by human eye). A decrease in turbidity can arise from dissociation of the higher, insoluble peptides to lower soluble ones, and/or from sedimentation of the higher insoluble peptides at the bottom of the measuring vial.

Finally, a general conclusion is drawn that in the α-amino acid solutions stored for the longer periods of time, peptidization progresses in a nonmonotonic fashion. Due to the randomness of size with peptide nano- and microparticles spontaneously formed in each individual experimental cycle, absolute turbidity values can change from one cycle to another, yet the shapes of individual turbidity patterns remain similar independent of the repetitions. Thus we can point out to the similarity of certain turbidity patterns and dissimilarity of the other ones, and speculate on spontaneous formation of the secondary α-heliceous peptide structures in the former case. It is understandable that in view of a lack of standardization in turbidity units, measurement devices and calibration techniques, usage of turbidimetry to analytical determinations can only be empirical and rather qualitative [23].

HPLC-ELSD

Due to specific nature of turbidimetric results which represent a sum of the light scattering effects with insoluble peptides of unknown yields, shapes, and molecular weights present in the investigated solutions, we cannot expect direct correlation thereof with chromatographic results which provide a quantitative insight in peptidization. However, certain analogies between turbidimetric and chromatographic results have been observed.

L-Ala, *D*-Ala, and *DL*-Ala solutions

For the *L*-, *D*-, and *DL*-Ala solutions, the chromatographic peak heights (corresponding to the monomeric Ala concentrations) were recorded in the course of the initial 12 h of samples ageing in the 10-min intervals, with the retention time value (t_R) equal to 3.5 min for each Ala sample. The obtained chromatographic time series are given in Fig. 3. The most important observation is that the plots shown in

Fig. 3 Time series of the chromatographic peak heights for (*i*) *L*-Ala, (*ii*) *D*-Ala, and (*iii*) *DL*-Ala solution in 70% aqueous methanol (registered over the course of 48 h)
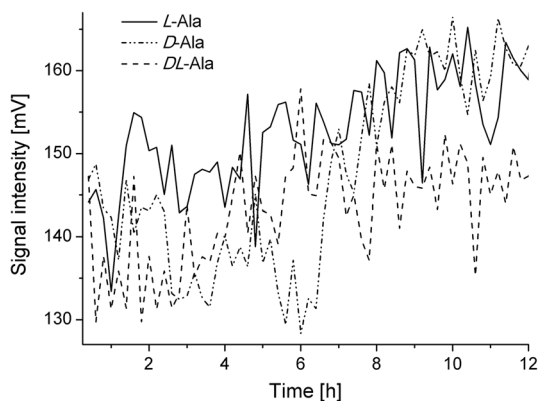
Fig. 3 directly confirm an oscillatory nature of the concentration changes with the monomeric Ala species and indirectly, the oscillatory nature of the peptides formation. High amplitudes of the respective concentration changes often equal to a dozen mV units. However, no similarity such, as synchronization of the oscillation dynamics along the time axis is observed among the time series patterns valid for *L*-, *D*-Ala, and *DL*-Ala.

L-Phe, *D*-Phe, and *DL*-Phe solutions

For the *L*-, *D*-, and *DL*-Phe solutions, the chromatographic peak heights (corresponding to the monomeric Phe concentrations) were recorded in the course of the initial two days of samples ageing in the 10-min intervals, with the retention time value (t_R) equal to 7.5 min for the *L*-, *D*-, and *DL*-Phe sample. The chromatographic time series are given in Fig. 4. The most important observation is that the plots shown in Fig. 4 directly confirm an oscillatory nature of the concentration changes with the monomeric Phe species and indirectly, the oscillatory nature of the peptides formation. Then a certain similarity is observed between the time series patterns valid for *L*- and *D*-Phe, whereas the time series pattern valid for *DL*-Phe is different. Similarity of the *L*- and *D*-Phe patterns consists in synchronization of the oscillation dynamics along the time axis and in high amplitudes of the respective concentration changes, often equaling to several dozen mV units. The time series pattern valid for *DL*-Phe does not show synchronization with the remaining two patterns and the amplitudes of the concentration changes in this latter case are in the range of *ca.* 10 mV only.

LC-MS

The main aim of the LC-MS analysis was to prove that in the binary α-amino acid systems, both homo- and heteropeptides are spontaneously formed. Four binary systems (*L*-Ala-*L*-Phe, *D*-Ala-*D*-Phe, *L*-Ala-*D*-Phe and *D*-Ala-*L*-Phe) were selected

Fig. 4 Time series of the chromatographic peak heights for (*i*) *L*-Phe, (*ii*) *D*-Phe, and (*iii*) *DL*-Phe solution in 70% aqueous methanol (registered over the course of 48 h)
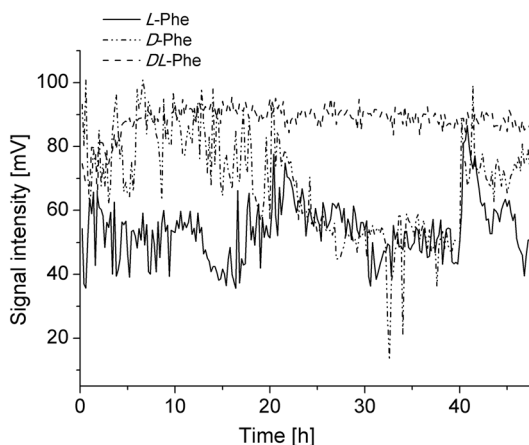
for this investigation and the respective mass spectra recorded. In each spectrum, signal originating from the monomeric Ala cation is registered (m/z 89.8, $[Ala + H]^+$), and in two spectra (L-Ala-L-Phe and L-Ala-D-Phe), signal originating from the monomeric Phe cation is also present (m/z 165.8, $[Phe + H]^+$). In L-Ala-L-Phe, three m/z signals at 350.5, 801.1, and 1867.1 are ascribed, respectively, to the homopeptide cations ($[Ph_7 + 3H]^{3+}$, $[Ala_{11} + H]^+$, and $[Ala_{26} + H]^+$), and six m/z signals are ascribed to the heteropeptide cations. In D-Ala-D-Phe, five m/z signals at 840.7, 871.2, 1342.9, 1452.4 and 1605.2 are ascribed, respectively, to the homopeptide cations ($[Ala_{47} + 4H]^{4+}$, $[Ala_{12}]^+$, $[Phe_9 + H]^+$, $[Ala_{61} + 3H]^{3+}$, and $[Ala_{22} + Na]^+$), and five m/z signals are ascribed to the heteropeptide cations. In L-Ala-D-Phe, three m/z signals at 350.5, 792.0, and 898.6 are ascribed, respectively, to the homopeptide cations ($[Phe_7 + 3H]^{3+}$, $[Ala_{25} + 2H]^{2+}$, and $[Phe_{16} + 3H]^{3+}$), and eight signals are ascribed to the heteropeptide cations. In D-Ala-L-Phe, one signal at m/z 1785.3 is ascribed to the homopeptide cation ($[Phe_{12} + H]^+$), and nine signals are ascribed to the heteropeptide cations. Summing up, the obtained mass spectra provide a convincing enough evidence of spontaneous formation of the homo- and heteropeptides in each analyzed binary α-amino acid system. The discussed mass spectra are available as a supplementary material.

We also reflect on molecular proportions between Ala and Phe in the heteropeptides formed in the inequichiral binary solutions. The m/z signals in L-Ala-D-Phe at 1389.4, 1470.6, 1821.3, and 1926.6 are ascribed to the $[Ala_{19} + Phe_{19} + 3H]^{3+}$, $[Ala_8 + Phe_6 + H]^+$, $[Ala_{15} + Phe_5 + H]^+$, and $[Ala_2 + Phe_{12}]^+$ cation. The m/z signals in D-Ala-L-Phe at 1281.6, 1475.9, 1633.1, 1983.5 are ascribed to the $[Ala_{13} + Phe_{11} + 2H]^{2+}$, $[Ala_6 + Phe_7 + H]^+$, $[Ala_{21} + Phe_{23} + 3H]^{3+}$, and $[Ala_9 + Phe_9 + H]^+$ cation, in order. In many of these heteropeptides, quantitative proportions between the two α-amino acids are either equal to 1:1 (e.g., 19:19), or quite close to this value (e.g., 8:6, 13:11, 21:23, etc.). Although in most cases considerably more than seven monomer units of one species (either Ala, or Phe) are involved, due to randomness of the assembling mechanism one can expect neither equichiral heptades, nor the resulting secondary α-helix structures.

Spectroscopy of far UV circular dichroism (CD)

The far UV circular dichroism performs well, when estimating secondary structures of globular proteins [32–34], yet the analysis of linear peptides is considerably more complicated [35] and mathematical algorithms have to be used to deconvolve the CD spectra in order to assess relative contributions from a variety of secondary structures (α-helices, β-sheets, coils etc.). However, we used the CD spectroscopic technique just to qualitatively compare the CD spectra in the range of 190 ÷ 260 nm (characteristic of the secondary linear peptide structures) for the systems composed of equichiral and inequichiral α-amino acid molecules after four months ageing. Respective CD spectra are presented in Figs. 5a–5f and we believe that the predominant contribution to these spectra originates from α-helices (as more complicated secondary structures are less probable as a result of spontaneous peptidization carried out for four months only.
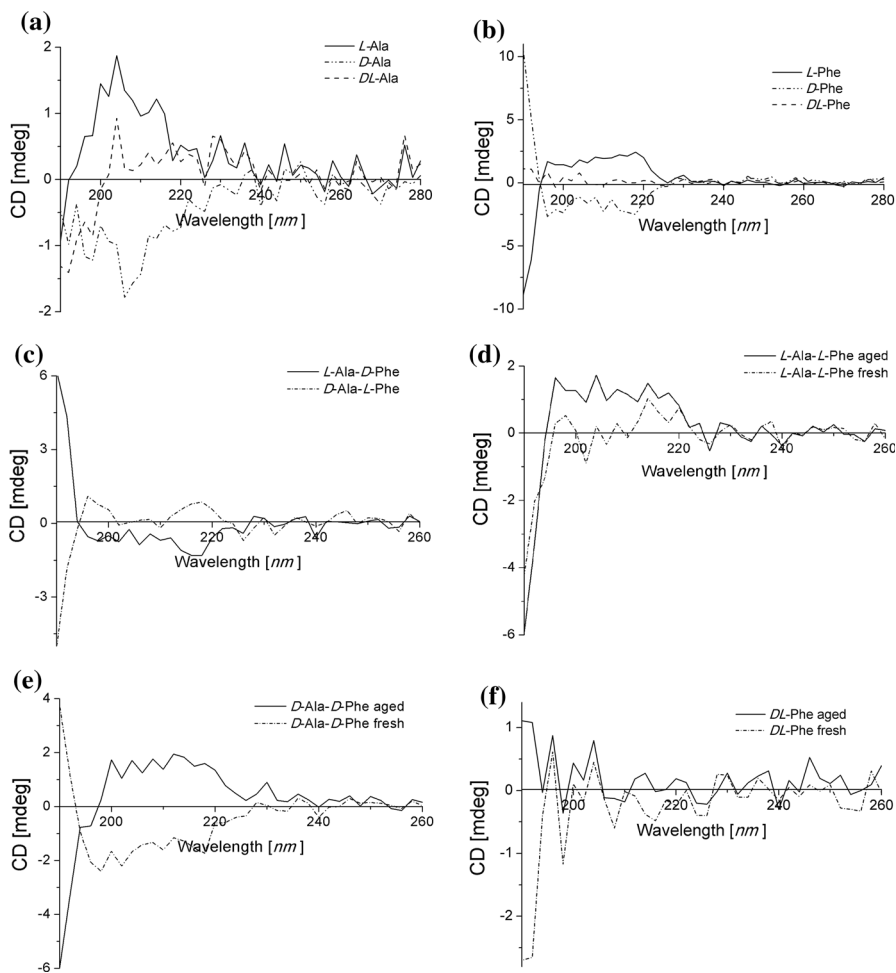
Fig. 5 CD spectra recorded for the solutions of **a** *L*-, *D*-, and *DL*-Ala, **b** *L*-, *D*-, and *DL*-Phe, and **c** *L*-Ala-*D*-Phe and *D*-Ala-*L*-Phe after the four months samples ageing, and for the fresh and aged solutions of **d** *L*-Ala-*L*-Phe, **e** *D*-Ala-*D*-Phe, and **f** *DL*-Phe (after the four months samples ageing)

In Fig. 5a, we compare the CD spectra for *L*-, *D*-, and *DL*-Ala. In the sample of *L*-Ala, two *Cotton* bands characteristic of α-helix can be seen with the first band positive and the second one negative. In the sample *D*-Ala, also two *Cotton* bands can be seen with the first band negative and the second band positive. The CD spectrum for the racemic (*DL*-Ala) sample is considerably less intense than the other two, with the first *Cotton* band positive and the second band negative. Thus, we assume that in the inequichiral (racemic) mixture, the *L*-Ala-derived α-helices predominate and *D*-Ala hardly participates in the helical secondary structures.

In Fig. 5b, we compare the CD spectra for *L*-, *D*-, and *DL*-Phe. For *L*-Phe, two *Cotton* bands can be seen with the first band positive and the second band negative. For *D*-Phe, two *Cotton* bands can be seen with the first band negative and the second

band positive. From the CD spectrum of the racemic (*DL*-Phe) sample, the *Cotton* bands are practically absent and hence, apparently no (or trace amounts) of equichiral α-helices are formed.

In Fig. 5c, we show the CD spectra for the two binary *L*-Ala-*D*-Phe and *D*-Ala-*L*-Phe samples, each one composed of two inequichirial α-amino acids. The spectrum valid for *L*-Ala-*D*-Phe shows two *Cotton* bands, the first band negative (characteristic of *D*-Phe) and the second band positive. Thus we assume that in the investigated sample, the *D*-Phe-derived α-helices are formed. The plot valid for *D*-Ala-*L*-Phe also demonstrates two *Cotton* bands, the first band positive (characteristic of *L*-Phe) and the second band negative. In this case, we assume that in the investigated sample, the *L*-Phe-derived α-helices are formed. Thus in the aged *L*-Ala-*D*-Phe and *D*-Ala-*L*-Phe systems, the observed signs of the respective *Cotton* bands point out to the selective formation of the Phe-derived α-helices, with the monomeric Ala units hardly engaged in the helical structures.

In Fig. 5d, we show CD spectra for the fresh and aged sample of the binary equichiral *L*-Ala-*L*-Phe system. The fresh sample demonstrates a very low intensity CD spectrum characterizing with the first *Cotton* band positive and the second band negative (characteristic of the *L* configuration of both α-amino acids). The reason for an appearance of these two *Cotton* bands in the fresh sample is not quite clear and it can either be due to trace contamination of the commercial monomeric α-amino acids with the peptides, or to fast peptidization upon dissolution. After four months of sample ageing, the intensity of the CD spectrum considerably grows, witnessing to peptidization progress and the higher yields of α-helices in the system.

The most interesting phenomenon is shown in Fig. 5e, which holds for the fresh and aged sample of the binary equichiral *D*-Ala-*D*-Phe system. The fresh sample demonstrates α-helix characterizing with the first *Cotton* band negative and the second band positive (pointing out to the *D* configuration of the amino acids involved). Again, the reason for its appearance in the fresh sample is not quite clear (either due to contamination of the commercial monomeric α-amino acids with certain amounts of peptides, or to fast peptidization upon dissolution). A striking phenomenon though is that after the four months storage period, the CD spectrum confirms the presence of the α-helical structures, yet with the reversed signs of the two *Cotton* bands, i.e., the first band is now positive and the second band is negative (pointing out to the *L* configuration of the amino acids involved). This result witnesses not only to the process of peptidization, but also to chiral conversion in the course of sample ageing.

One more interesting example is furnished by Fig. 5f, which holds for the fresh and aged sample of the racemic *DL*-Phe system. In this case, the intensities of the two plots in the range of 190 ÷ 260 nm are almost negligible (and especially in the range of the first *Cotton* band), which confirms negligible amounts of the α-helix structures only. However, in the range of the second *Cotton* band the negative slope for the fresh sample changes to the positive slope for the aged sample. This result also seems indicative of the process of chiral conversion taking place in the system in the course of sample storage.

Summing up, the CD spectroscopic results confirm spontaneous formation of α-helical secondary structures in the equichiral *L*, *D*, *L-L*, and *D-D* systems on the one

hand, and either an inability to form α-helices in the inequichiral *DL* system (Figs. 5b and 5f), or the formation of α-helical homochiral peptides in the binary *D-L* systems (Figs. 5a and 5c). In this sense, the obtained CD results support our assumptions derived from turbidimetric data and presented earlier. An additional gain of applying the CD spectroscopy is confirmation with its aid of the processes of chiral conversion.

Conclusions

The non-linear turbidity changes with the monocomponent and binary Ala and Phe solutions are due to the oscillatory peptidization process which results in the formation of insoluble higher molecular weight peptides, extensively discussed elsewhere. In this study, the similarity of turbidity patterns is in the main focus of our attention. It is tentatively ascribed to equichirality of all α-amino acid units in a molecule of a given peptide and consequently, to a possible formation of the peptide α-helix structure. Analogously, the dissimilarity of turbidity patterns is tentatively explained by inequichirality of α-amino acid units in the respective peptides. However, the formation of peptide α-helices is regarded as a working hypothesis only, conceived by equichirality of the monomeric units involved and the other molecular level mechanisms leading to the secondary peptide structures cannot be excluded, which might eventually complement or replace the α-helix concept. The HPLC-ELSD data confirm the non-linear nature of peptidization and certain analogies are emphasized between the turbidimetric and chromatographic results. The MS data confirm formation of peptides, and the CD data confirm a possibility of formation of α-helical structures in equichiral α-amino acid systems.

References

1. Sajewicz M, Matlengiewicz M, Leda M, Gontarska M, Kronenbach D, Kowalska T, Epstein IR (2010) Spontaneous oscillatory in vitro chiral conversion of simple carboxylic acids and its possible mechanism. J Phys Org Chem 23:1066–1073
2. Sajewicz M, Gontarska M, Kronenbach D, Leda M, Kowalska T, Epstein IR (2010) Condensation oscillations in the peptidization of phenylglycine. J Syst Chem 1:7. doi:10.1186/1759-2208-1-7
3. Sajewicz M, Godziek A, Maciejowska A, Kowalska T (2015) Condensation dynamics of the *L*-Pro-*L*-Phe and *L*-Hyp-*L*-Phe binary mixtures in solution. J Chromatogr Sci 53:31–37

4. Sajewicz M, Piętka R, Pieniak A, Kowalska T (2005) Application of thin-layer chromatography (TLC) to investigating oscillatory instability of the selected profen enantiomers. Acta Chromatogr 15:131–149

5. Sajewicz M, Gontarska M, Wróbel M, Kowalska T (2007) Enantioseparation and oscillatory transenantiomerization of S, R-(±)-ketoprofen, as investigated by means of thin layer chromatography with densitometric detection. J Liq Chromatogr Relat Technol 30:2193–2208

6. Sajewicz M, Kronenbach D, Gontarska M, Wróbel M, Piętka R, Kowalska T (2009) TLC in search for structural limitations of spontaneous oscillatory in vitro chiral conversion. α-hydroxybutyric and mandelic acids. Planar Chromatogr-Modern TLC 22:241–248

7. Sajewicz M, Dolnik M, Kronenbach D, Gontarska M, Kowalska T, Epstein IR (2011) Oligomerization oscillations of L-lactic acid in solutions. J Phys Chem A 115:14331–14339

8. Adler-Abramovich L, Reches M, Sedman VL, Allen S, Tendler SJB, Gazit E (2006) Thermal and chemical stability of diphenylalanine peptide nanotubes: implications for nanotechnology applications. Langmuir 22:1313–1320

9. Ryu J, Park CB (2010) High stability of self-assembled peptide nanowires against thermal, chemical and proteolytic attacks. Biotechnol Bioeng 105:221–230

10. Reches M, Gazit E (2004) Formation of closed-cage nanostructures by self-assembly of aromatic dipeptides. Nano Lett 4:581–585

11. Görbitz CH (2006) The structure of nanotubes formed by diphenylalanine, the core recognition motif of Alzheimer's beta-amyloid polypeptide. Chem Commun (Camb) 22:2332–2334

12. Maltsev AV, Bystryak S, Galzitskaya O (2011) The role of β-amyloid peptide in neurodegenerative diseases. Ageing Res Rev 10:440–452

13. Tokunaga M, Liu ML, Nagai T (2010) Implantation of cardiac progenitor cells using self-assembling improves cardiac function after myocardial infarction. J Mol Cell Cardiol 49:972–983

14. Ueda Y, Ishii K, Toyama Y, Nakamura M, Okano H (2008) Transplantation of human neural stem cells for spinal cord injury in primates. Neurosci Res 1:93–93

15. Debnath S, Roy S, Ulijn RV (2013) Peptide nanofibers with dynamic instability through nonequilibrium bioanalytic assembly. J Am Chem Soc 135:16789–16792

16. Samaritoni JG, Copes AT, Crews DeMarcus K (2014) Unexpected hydrolytic instability of N-acylated amino acid amides and peptides. J Org Chem 79:3140–3151

17. Villani V, Tamburro AM, Comenges JMZ (2000) Conformational chaos and biomolecular instability in aqueous solution. J Chem Soc, Perkin Trans 2:2177–2184

18. Godziek A, Maciejowska A, Sajewicz M, Kowalska T (2015) HPLC monitoring of spontaneous nonlinear peptidization dynamics of selected amino acids in solution. J Chromatogr Sci 53:401–410

19. Sajewicz M, Matlengiewicz M, Juziuk M, Penkala M, Weloe M, Schulz M, Kowalska T (2013) Thin-layer chromatographic evidence of proline peptidization in solution and its thin-layer chromatographic enantioseparation. J Liq Chromatogr Relat Technol 36:2497–2511

20. Godziek A, Maciejowska A, Talik E, Wrzalik R, Sajewicz M, Kowalska T (2016) On spontaneously pulsating proline-phenylalanine peptide microfibers. Curr Protein Pept Sci 17:106–116

21. Kowalska T, Sajewicz M (2016) Possibilities and limitations of selected analytical tools to trace nonlinear chemical processes. In: Proceedings of the 13th international conference on fundamental and applied aspects of physical chemistry "Physical Chemistry 2016", Belgrade, Serbia, September 26th–30th, 2016

22. Maciejowska A, Godziek A, Talik E, Sajewicz M, Kowalska T (2015) Investigation of spontaneous chiral conversion and oscillatory peptidization of L-methionine by means of TLC and HPLC. J Liq Chromatogr Relat Technol 38:1164–1171

23. Lawler DM (2005) Turbidity and nephelometry. In: Worsfold P, Townshend A, Poole C (eds) Encyclopedia of analytical science, 2nd edn. Elsevier Academic, San Diego, USA, pp 343–352

24. Lawler DM, Brown RM (1992) A simple and inexpensive turbidity meter for the estimation of suspended sediment concentrations. Hydrol Proc 6:159–168

25. Maciejowska A, Godziek A, Talik E, Sajewicz M, Kowalska T, Epstein IR (2016) Spontaneous pulsation of peptide microstructures in an abiotic liquid system. J Chromatogr Sci 17:106–116

26. Baldwin RL (2003) In search of the energetic role of peptide hydrogen bonds. J Biol Chem 278:17581–17588

27. Mortishire-Smith RJ, Drake AF, Nutkins JC, Williams DH (1991) Left handed α-helix formation by a bacterial peptide. FEBS Lett 278:244–246

28. Lins RD, Ferreira R (2006) The stability of right- and left-handed alpha-helices as a function of monomer chirality. Quim Nova 29:997–998

29. Maciejowska A, Godziek A, Sajewicz M, Kowalska T (2017) Circadian rhythm of spontaneous non-linear peptidization with proteinogenic amino acids in abiotic solutions versus homochirality. Acta Chromatogr 29:135–142

30. Blout ER (1962) The dependence of the conformation of polypeptides and proteins upon of amino acid composition. In: Stahmann MA (eds) Polyamino acids, polypeptides, and proteins. The University of Wisconsin Press, Madison, WI, USA, pp 275–279

31. Gruber M, Lupas AN (2003) Historical review. Another 50th anniversary. New periodicities in coiled coils. Trend Biochem Sci 28:679–685

32. Provencher SV, Glöckner J (1981) Estimation of globular protein secondary structure from circular dichroism. Biochemistry 20:33–37

33. Hennesey JP, Johnson WC (1981) Information content in the circular dichroism of proteins. Biochemistry 20:1085–1094

34. Perczel A, Foxman BM, Fasman GD (1992) How reverse turns may mediate the formation of helical segments in proteins: an x-ray model. Proc Natl Acad Sci USA 89:8210–8214

35. Reed J, Reed TA (1997) A set of constructed type spectra for the practical estimation of peptide secondary structure from circular dichroism. Anal Biochem 254:36–40